11th World Congress on Computational Mechanics (WCCM XI)
5th European Conference on Computational Mechanics (ECCM V)
6th European Conference on Computational Fluid Dynamics (ECFD VI)
E. Oñate, J. Oliver and A. Huerta (Eds)

ON THE CONTROL OF SPURIOUS FORCE OSCILLATIONS FOR MOVING BODY PROBLEMS USING AN IMMERSED BOUNDARY METHOD

M. BELLIARD[◇,*], M. CHANDESRIS[◇,†], J. DUMAS[◇,‡], Y. GORSSE[◇,*], D. JAMET[◇,‡] AND C. JOSSERAND[♮]

[◇] Commissariat à l'Énergie Atomique et aux Énergies Alternatives, CEA, DEN/DANS/DM2S/STMF/LMEC

[*]CEA Cadarache, bâtiment 238, F-13108 Saint Paul-lez-Durance, France, michel.belliard@cea.fr, yannick.gorsse@cea.fr

[†] CEA Grenoble, bâtiment 10.05, F-38054 Grenoble Cedex, France

[‡] CEA Saclay, bâtiment 454, Route Nationale, F-91400 Gif-sur-Yvette Cedex, France

[♮] Institut Jean le Rond d'Alembert, Université, Pierre et Marie Curie, Tour 55-65, 4 place Jussieu, F-75252 Paris Cedex 05, France

Key words: Immersed Boundary Method, Moving Bodies, Spurious Force Oscillations, Fluid Structure Interaction

Abstract. We present a Direct Forcing (DF) approach for simulations of flows over moving bodies, on Cartesian grids, capable of reducing the amplitude of the force oscillations, by using a regularized approach.

1 INTRODUCTION

Fluid-structure interaction (FSI) problems are tricky to simulate due to the complexity of the physical phenomena and the presence of time varying geometries. In the well-known body-fitted approach the boundary conditions (BC), that are critical for FSI issues, are exactly imposed on the physical domain boundary. However accurate this approach may be, it is sometimes difficult to deal with the re-meshing issue, specially for large fluid-mesh deformations. Another approach consists in using immersed boundary methods (IBM) [1]. The general idea is to consider only a fluid domain in which the solid boundaries are immersed. We recover the immersed BC by adding a supplementary term in the governing equations of the fluid, referred to as the forcing term. Here, we consider the Direct Forcing (DF) method [2] that is particular discrete version of the IBM for rigid

solids. This method has been successfully applied to various problems [3]. Unfortunately, one undesirable property is the generation of spurious force oscillations (SFO) [4, 5, 6] when dealing with moving bodies on a fixed computational grid.
Here, we present a Regularized Direct Forcing (RDF) approach [7] for simulations of flows over moving bodies capable of reducing the amplitude of the SFO. We have identified the primary source of these oscillations as the temporal discontinuity of the forcing term across the fluid-solid interface, concerning mainly the dead cells. Indeed, when the velocity point comes near the solid boundary, the original DF approach consists in forcing the previously computed fluid velocity to a prescribed one. Therefore the forcing term is highly discontinuous in time for dead cells leading to the famous spurious force oscillations. In the proposed RDF approach, this prescribed fluid velocity is chosen in a such a way that the magnitude of the forcing term tends to zero with the inverse of the distance to the immersed interface (or with the solid volume fraction). By modifying the definition of the prescribed fluid velocity, it is possible to change the order of approximation of the method. A first order and a second order version of the method are presented here.
The results obtained with the present RDF approach are similar to those obtained with much more complicated method [8, 6, 9]. Moreover our method is very easy to implement, effective and improve the numerical precision by comparison with the original DF approach.

2 NUMERICAL METHODS

The governing equations used to describe unsteady incompressible flows are the incompressible Navier-Stokes (NS) equations -here with Dirichlet BCs for the sake of the presentation-:

$$\begin{aligned} \frac{\partial \underline{u}}{\partial t} + \nabla \cdot (\underline{u} \otimes \underline{u}) + \frac{1}{\rho}\underline{\nabla} p - \nu \nabla^2 \underline{u} &= \underline{g} \quad \text{in } \Omega \\ \nabla \cdot \underline{u} &= 0 \quad \text{in } \Omega \\ \underline{u} &= \underline{u}_D \text{ on } \partial\Omega \end{aligned} \tag{1}$$

where Ω is the computational domain, $\partial\Omega$ its boundary, $\underline{u}$ the fluid velocity, ν the kinematic viscosity, p the pressure, ρ the fluid density and $\underline{g}$ bulk forces. A non-incremental fractional-step scheme is used to solve the governing equations (1) [10, 11].

Following the IBM developed by [2], the computational domain Ω corresponds to a uniform Eulerian grid including the fluid domain Ω_F and the embedded solid domain Ω_S such as $\Omega = \Omega_F \cup \Omega_S$. The presence of embedded time-varying geometry Ω_S is taken into account thanks to a source term $\underline{F}_{DF}$, added to the time semi-discretized form of the Navier-Stokes Eqs. (1). For instance, with an explicit Euler scheme and considering

a projection solver, this is done in two steps:

$$\frac{\underline{u}^\star - \underline{u}^n}{\Delta t} + \nabla \cdot (\underline{u}^n \otimes \underline{u}^n) + \underline{\nabla} P^n - \nu \nabla^2 \underline{u}^n \quad = \quad \underline{g} \text{ in } \Omega, \tag{2}$$

with $\underline{u}^\star$ a predicted velocity without taken into account the immersed boundary Σ. This step depends on the time scheme. The forcing step is:

$$\underline{\tilde{u}} \quad = \quad \underline{u}^\star + \Delta t \underline{F}_{DF} \tag{3}$$

where $\underline{\tilde{u}}$ is the predicted velocity that satisfies the IBC and Δt the time step. Finally, the projection and the correction steps remain classical:

$$\frac{1}{\rho} \Delta p^{n+1} \quad = \quad \frac{1}{\Delta t} \nabla \cdot \underline{\tilde{u}} \text{ in } \Omega \tag{4}$$

$$\underline{u}^{n+1} = \underline{\tilde{u}} - \frac{\Delta t}{\rho} \underline{\nabla} p^{n+1} \text{ in } \Omega. \tag{5}$$

The source term $\underline{F}_{DF}$ is defined by:

$$\underline{F}_{DF} = \chi_{\mathrm{m}} \frac{\underline{u_i} - \underline{u}^\star}{\Delta t} \text{ in } \Omega \tag{6}$$

where $\underline{u_i}$ is the imposed fluid velocity and χ_{m} is the phase indicator function of the imposed velocity domain Ω_I^{m}:

$$\chi_{\mathrm{m}}(\underline{x}) = \begin{cases} 1 & \text{for } \underline{x} \in \Omega_I^{\mathrm{m}} \\ 0 & \text{otherwise.} \end{cases} \tag{7}$$

where $\underline{x}$ is the position. The imposed fluid velocity can be obtained by interpolations of various orders from the BC and the fluid velocity. Here we consider interpolations of order 1 (base model: the imposed velocity is equal to the solid one $\underline{u}_D$) and of order 2 (linear model: linear interpolation [12]).

The space discretization is based on a finite volume approximation with a staggered grid arrangement of the variables $(\underline{u}, P)$. As a result, the pressure degrees of freedom are located at the cell centers whereas those of each velocity component are placed at the middle of the cell edges. The governing Eqs. (1) are integrated over each control volume ensuring the conservation of mass and momentum balance. The convection and diffusion terms are respectively approached by the QUICK and centered schemes.

3 ANALYZE OF THE SFO

Let us consider the test case of Seo and Mittal [6] as sandbox. It consists in a circular cylinder of diameter D oscillating along the x-direction in a fluid at rest:

$$\begin{aligned} x_c(t) &= x_c(0) + X_0(1 - cos(2\pi f_0 t)) \\ y_c(t) &= y_c(0) \end{aligned} \tag{8}$$

where $(x_c(0), y_c(0))$ are the initial coordinates of the cylinder center, X_0 the amplitude of the oscillations and their frequency f_0, see the Fig. 1(a). Fig. 1(b) shows the evolution over a period T_0 of the dimensionless coefficients concerning the pressure drag C_P, the friction drag C_ν, the total drag C_T and the total contribution of the direct forcing term $C_{DF} = \frac{\iiint_{\Omega_S} \rho \underline{F}_{DF} \cdot \underline{e}_x \mathrm{d}\Omega}{\underline{F}_{ref} \cdot \underline{e}_x}$ with $\underline{F}_{ref}$ a scaling vector and $\underline{e_x}$ the x-direction unit vector.

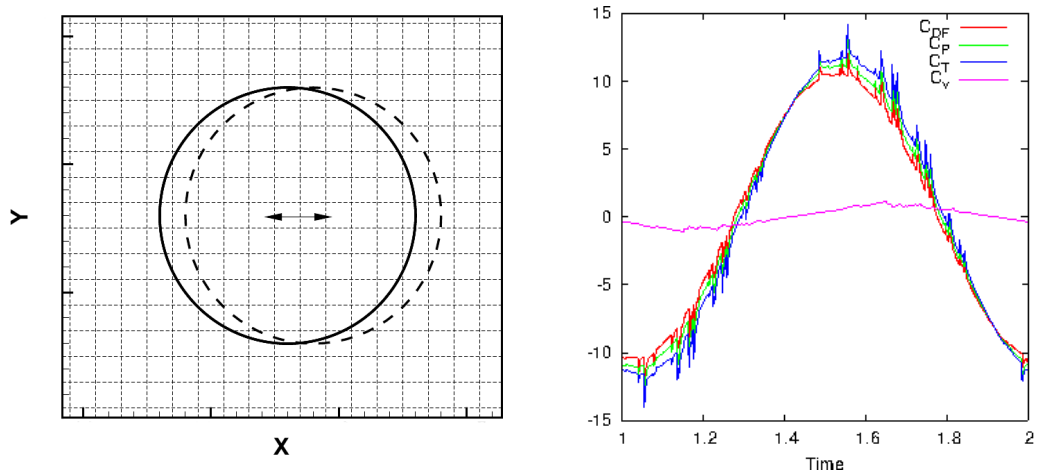

(a) (b)

Figure 1: Mittal's test case 1(a) geometry and computational grid. Physical dimensionless coefficients time histories: C_P, C_ν, C_T and C_{DF}.

Mainly, it is the pressure drag component that is disturbed by the spurious oscillations whereas the time history of the friction drag is almost regular. Therefore, the SFO are in fact due to the spurious pressure oscillations (SPO). It is also interesting to notice that C_{DF} is nearly equal to C_T.

Analyzing the SPO origin in the case of the DF base model, we obtain under reasonable hypothesis [7] that the measure of the DF term variation between the time steps n and $n+1$ can be approached by:

$$\begin{aligned} \int_{\Omega_{s,h}^{n+1}} \underline{F}_{DF}^{n+1} \mathrm{d}\Omega - \int_{\Omega_{s,h}^{n}} \underline{F}_{DF}^{n} \mathrm{d}\Omega &= \underbrace{\mathcal{O}(1)}_{K \in \Omega_{s,h}^{n+1} \cap \Omega_{s,h}^{n}} + \underbrace{\mathcal{O}(\Delta x) + \mathcal{O}(\frac{\Delta x^2}{\Delta t})}_{K \in DC} + \underbrace{\mathcal{O}(\Delta x)}_{K \in FC} \\ &= \mathcal{O}(1) + \mathcal{O}(\Delta x) + \mathcal{O}(\frac{\Delta x^2}{\Delta t}) \end{aligned} \quad (9)$$

where Δx is the space step, $\Omega_{s,h}^{n*}$ is the imposed velocity domain at time $n*$, the FC (fresh cells) is the set of velocities that became freshly fluids ($K \in \Omega_{s,h}^{n} \setminus \Omega_{s,h}^{n+1}$) and DC (dead cells) the set of velocities that became freshly forced ($K \in \Omega_{s,h}^{n+1} \setminus \Omega_{s,h}^{n}$). This

equation implies that the SPO decrease with decreasing the grid spacing and increasing the computational time step. The exponents are in good agreement with [6]. Additional studies conclude that the DC are the main source of pressure oscillations, cf. Fig. 2 [7].

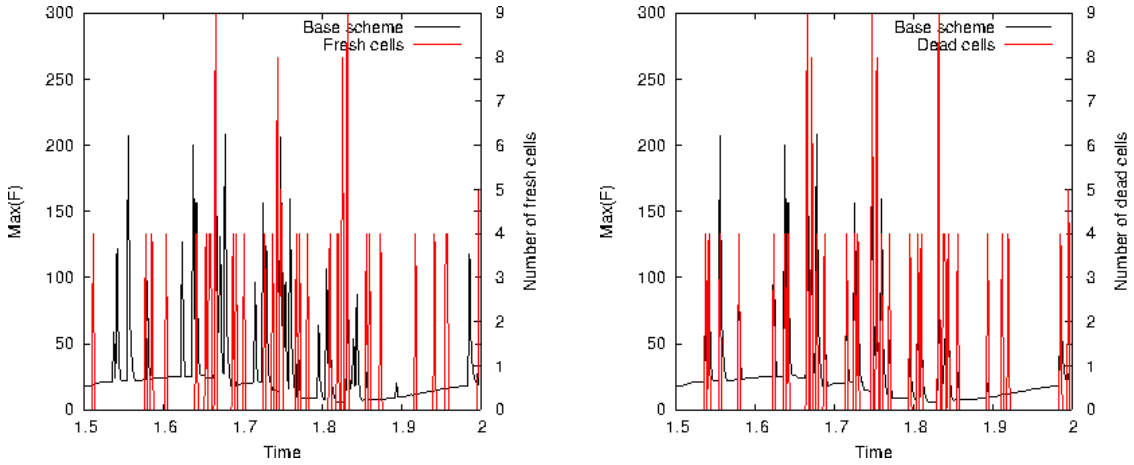

(a) (b)

Figure 2: Forcing term maximum on the Mittal's test case. FC and DC numbers on the left and right sides.

4 REGULARIZED DIRECT FORCING

The classical DF method consists in modeling χ_{m} in consistence with a sharp transition of the forcing term at the forced-free interface, cf. Eq. (7). When a fluid point is reached by the solid boundary, we shapely jump from a velocity computed by the Navier-Stokes numerical scheme to a geometrical interpolation. Then the forcing term is highly discontinuous in time for the dead cells.
The key idea of the regularized DF formulation is to smooth this transition by replacing χ_{m} with a smoother function. The following formulation is proposed for the imposed velocity:

$$\underline{u_i} \quad = \quad \tau_{\mathrm{m}} \underline{u}_{\mathrm{m}} + (1 - \tau_{\mathrm{m}}) \underline{u}^{\star} \tag{10}$$

with $\underline{u}_{\mathrm{m}}$ is the interpolated velocity and τ_{m} is a smooth function of the distance to the immersed boundary Σ. For instance, τ_{m} can be the fraction of the forced-domain volume to the control volume associated with the fluid velocity.
Hence we force the velocity proportionally to τ_{m} in order to have a smooth transition: the fluid velocity will be forced progressively to the forced velocity as it enters in the forced domain. This formulation does not increase the computational time cost and is very easy to implement. We named it "regularized" (R) DF because the imposed velocity is a linear

combination of the NS computed velocity and the imposed interpolated velocity leading to a imposed regularized velocity.

For your tests we choose the following model for τ_{m}:

$$\underline{u}_i = \begin{cases} \underline{u}_{\mathrm{m}} & \text{if } \tau_{\mathrm{m}} = 1 \\ \tau_{\mathrm{m}}\underline{u}_{\mathrm{m}} + (1-\tau_{\mathrm{m}})\underline{u}^{\star} & \text{if } 0 < \tau_{\mathrm{m}} < 1 \\ \underline{u}^{\star} & \text{if } \tau_{\mathrm{m}} = 0 \end{cases} \tag{11}$$

with τ_m computed thanks to the distance function. It varies linearly with the distance from 0 to 1 across a layer of thickness Δx centered on the forced-free interface, see Fig. 3.

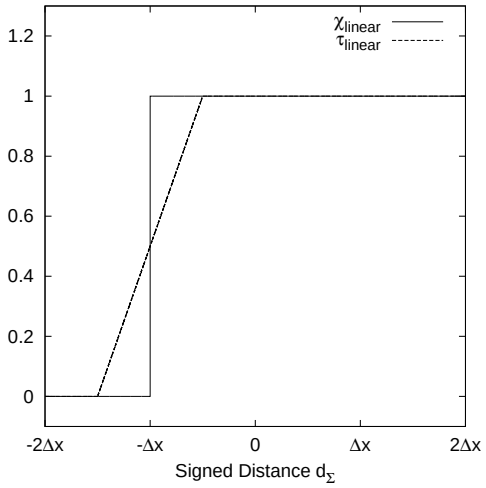

Figure 3: Representation of χ_{m} and τ_{m} for the classical DF method and the Regularized DF one.

Applying similar analysis than done in Section 3, we now obtain that the measure of the DF term variation between the time steps n and $n+1$ can be approached by:

$$\begin{aligned} \int_{\Omega_{s,h}^{n+1}} \underline{F}_{RDF}^{n+1} \mathrm{d}\Omega - \int_{\Omega_{s,h}^{n}} \underline{F}_{RDF}^{n} \mathrm{d}\Omega &= \underbrace{\mathcal{O}(1) + \mathcal{O}(\Delta t) + \mathcal{O}(\Delta x)}_{K \in \Omega_{s,h}^{n+1} \cap \Omega_{s,h}^{n}} + \underbrace{\mathcal{O}(\Delta t) + \mathcal{O}(\Delta x)}_{K \in DC} + \underbrace{\mathcal{O}(\Delta t)}_{K \in FC} \\ &= \mathcal{O}(1) + \mathcal{O}(\Delta t) + \mathcal{O}(\Delta x) \end{aligned} \tag{12}$$

Hence, the $\mathcal{O}(\frac{\Delta x^2}{\Delta t})$ term of Eq. (9) is reduced to $\mathcal{O}(\Delta x)$.

5 NUMERICAL APPLICATIONS

To demonstrate the effectiveness of the present DF forcing approach, in comparison with the original one, we restrict ourselves to only two classic moving-body problems from the literature. More validations examples can be found in [7].

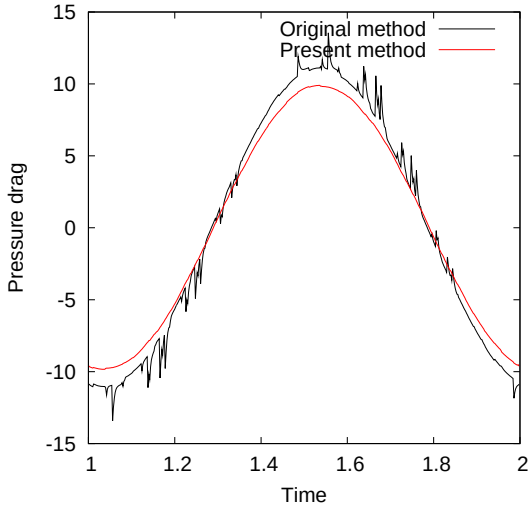

Figure 4: Time evolution of the pressure drag for an oscillating cylinder, test case from [6], using the original method and the present method, both with the first order version.

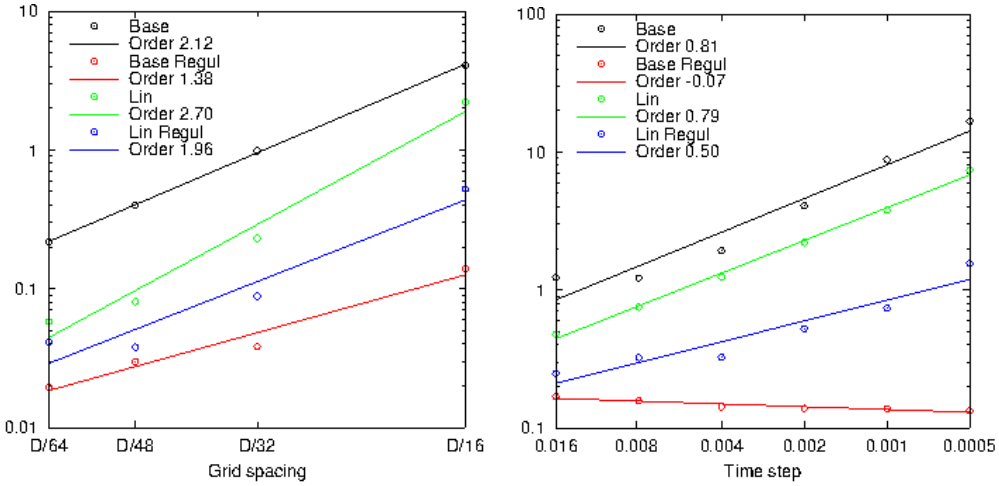

(a) Grid spacing convergence of the oscillations

(b) Time-step convergence of the oscillations

Figure 5: $Cp^{2\delta}_{Max}$ for the base and the linear interpolation schemes for both the DF and RDF formulations. The CFL number is set to 1.

The first test case is again from [6] where we consider an oscillating cylinder in a fluid at rest. The force oscillations are almost entirely suppressed for this test case, cf Fig. 4.

We used the pressure 2δ-discontinuity $C_P^{2\delta}$ [6] to quantitatively describe the SPO:

$$C_P^{2\delta} = C_P^{n+1} - 2C_P^n + C_P^{n-1} \tag{13}$$

where n is the time-step index. Space-step and time-step convergence studies of the amplitude of the SPO, cf. Fig. 5, conclude to a big damping of the SPO and corroborate the theoretical analysis.

Concerning the second test case, it consists in one of the numerical experiments conducted by E. Guilmineau and P. Queutey [13]: a circular cylinder with an imposed harmonic motion in a flow characterized by the Reynolds number $Re = \frac{UD}{\nu} = 185$. The imposed sinusoidal motion is defined by:

$$\begin{aligned} x_c(t) &= x_c(0) + A_e cos(2\pi f_e t) \\ y_c(t) &= y_c(0) \end{aligned} \tag{14}$$

where $(x_c(0), y_c(0))$ are the initial coordinates of the cylinder, A_e the amplitude of the oscillations and f_e their frequency. Here we have $A_e/D = 0.2$ and $f_e/f_0 = 1.1$ with D the diameter and f_0 the natural shedding frequency from the stationary cylinder.

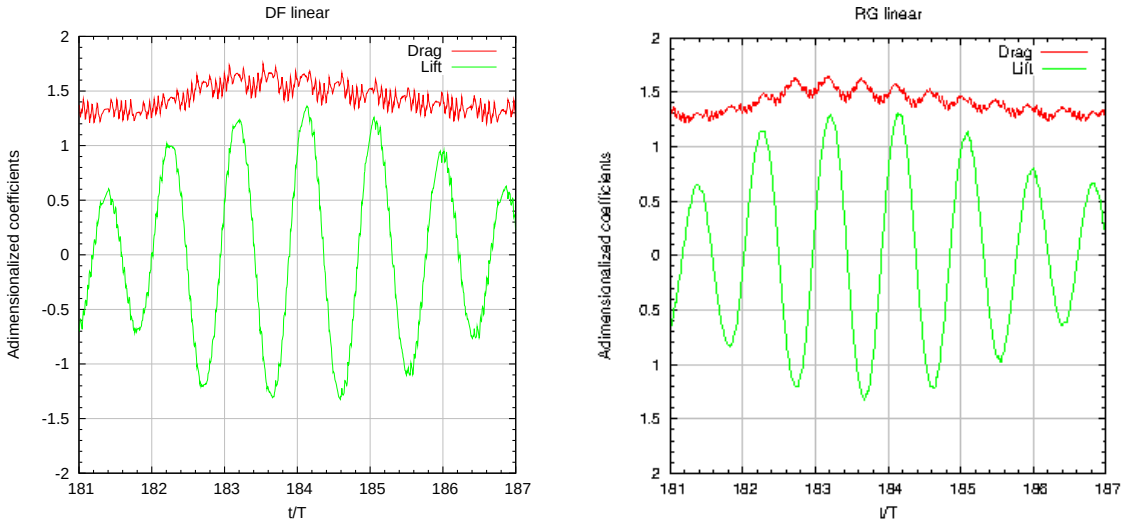

(a) (b)

Figure 6: Time history of the drag and lift coefficients over a period of time for the DF linear 6(a) and the RDF linear 6(b) formulations with a computational domain of $L/D = 60$ and a grid spacing ratio of $D/\Delta x = 12.5$.

Here again, the present RDF approach decreases the amplitude of the oscillations by almost one order of magnitude without altering the physics, cf. Fig. 6. Moreover, in Fig. 7, we qualitatively compare the drag and lift coefficients obtained by the RDF method equipped with linear interpolations to the Guilmineau results. The agreement is quite good.

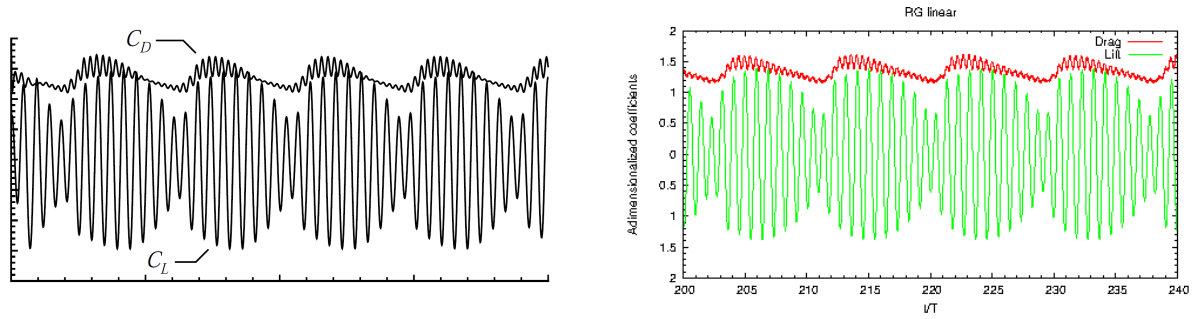

(a) (b)

Figure 7: Comparison of the drag and lift coefficients over a few periods of time, the picture 7(a) is comes from the article of E. Guilmineau [13] and 7(b) is the RDF linear formulation with a computational domain of $L/D = 60$ and a grid spacing ratio of $D/\Delta x = 25$.

6 CONCLUSIONS

The main goal of this paper was to present a new regularized direct forcing (RDF) approach capable of cutting off the SFO observed in simulations of moving boundary problems with sharp-interface IBM. The expression of the DF forcing term is carefully chosen to smooth the fluid temporal discontinuity through the fluid-solid interface, whatever is the order of the geometrical interpolation involved. This regularization process is quite general and can be adapted to the penalized direct forcing [12]. Consequently, it is possible to control and manage the magnitude of the spurious force oscillation. Moreover, theoretical analysis were performed to estimate the temporal variation of the forcing term for both the DF and the RDF methods in order to assess the spatial and time dependencies of the oscillations amplitude.

In order to illustrate the capacities of our method, two test cases were provided. One is an oscillating cylinder in a fluid at rest [6]. The other one is a cylinder with an imposed sinusoidal motion subjected to a cross-flow of Reynolds number 185 [13]. Both test case studies conclude to the drastic reduction of the SFO and the agreement of the spatial and time dependencies of the oscillations amplitude with our theoretical estimations.

From a general point of view, the RDF approach enables to decrease the spurious oscillations by at least one order of magnitude over a large range of grid spacing and time-step without increasing the computational cost. The results obtained in this matter are quite similar to [6] that used a cut cell method that is much more complicated to implement. It brings the possibility to accurately simulate full fluid structure interaction problems, such as flow induced vibration, without parasite fluctuation at the fluid-solid interface.

REFERENCES

[1] Peskin C. Numerical Analysis of blood flow in heart. *J. of Comput. Phys.* (1977) **25**:220-252.

[2] Mohd-Yussof J. Combined Immersed Boundaries/B-Splines Methods for Simulations of Flows in Complex Geometries. *CTR Annual Research Briefs, NASA Ames/Stanford University* (1997).

[3] Fadlun E. A., Verzicco R., Orlandi P. and Mohd-Yussof J. Combined immersed-boundary finite-difference for three-dimensional complex flow simulations. *J. of Comput. Phys.* (2000) **161**:35-60.

[4] Yang X., Zhang X., Li Z. and He G. A smoothing technique for discrete delta functions with application to immersed boundary method in moving boundary simulations. *J. of Comput. Phys.* (2009) **228**:7821-7836.

[5] Liao C.-C., Chang Y.-W., Lin C.-A. and McDonough J.M. Simulating flows with moving rigid boundary using immersed-boundary method. *Computers & Fluids* (2010) **39**:152-167.

[6] Seo J.H. and Mittal R. A sharp-interface immersed boundary method with improved mass conservation and reduced spurious pressure oscillations. *J. Comput. Phys.* (2011) **230**:7347–7363.

[7] Belliard M., Chandesris M., Dumas J., Gorsse Y., Jamet D. and Josserand C. A regularized formulation of direct forcing IBM to control spurious force oscillations in order to simulate complex fluid structure interaction problems. *Submitted* (2014).

[8] Lee J., Kim J., Choi H. and Yang K.S. Sources of spurious force oscillations from an immersed boundary method for moving-body problems. *J. Comput. Phys.* (2011) **230**:2677–2695.

[9] Lee J. and You D. An implicit ghost-cell immersed boundary method for simulations of moving body problems with control odd spurious force oscillations. *J. Comput. Phys.* (2013) **233**:295–314.

[10] Chorin A.J. Numerical solution of the Navier-Stokes equations. *Math. Comput.* (1968) **22**:745-762.

[11] Temam R. Sur l'approximation de la solution des équations de Navier-Stokes par la méthode des pas fractionnaires. *Arch. Rational Mech.* (1969) **32**:135-153.

[12] Introïni C., Belliard M., Fournier C. A second order penalized direct forcing for hybrid Cartesian/immersed boundary flow simulations. *Computers and fluids.* (2014) **90**:21-41.

[13] Guilmineau E. and Queutey P. A numerical simulation of vortex shedding from an oscillating circular cylinder. *J. Fluids and Structures* (2002) **16**:773–794.